

High-Temperature Oxidation Behavior of a New Ni-Cr-Mo-Si Alloy

B. A. Baker and G. D. Smith
Special Metals Corp.
3200 Riverside Drive
Huntington, WV 25705

B. A. Pint and L. R. Walker
Oak Ridge National Laboratory
1 Bethel Valley Road
Oak Ridge, TN 37831

ABSTRACT

The oxidation behavior of a new Ni-Cr-Mo-Si alloy has been evaluated from 1000°C to 1200°C in air plus 5% water vapor and in oxygen at 1200°C, under cyclic conditions. For comparison, two commercial and two experimental Ni-Cr-Si-Nb alloys and alloys HX, 600 and MA758 were included. The experimental results show that the Ni-Cr-Mo-Si material has excellent resistance to oxidation attack, provided by both a continuous chromium oxide scale, a discontinuous silicon oxide sub-scale, and rare-earth additions. Sample characterization methods include light and SEM microscopy and EPMA.

Keywords: Nickel-base alloys, oxidation, silicon oxide, chromium oxide, rare earth addition

INTRODUCTION

As thermocouple material development has progressed to improve temperature range capability and stability, the need for new sheathing materials matching the life of the thermocouple material has arisen as well. For high temperatures, some commonly used thermocouple sheathing materials have included: INCONEL® alloy 600, alloy HX and alloys TB and TC.[§] In this paper the high temperature oxidation properties of a new alloy, INCOTHERM™ alloy TD, will be compared to these other commonly used sheathing materials. Comparison with two additional Ni-Cr alloys, MA758 and 601, were included for

[§] INCONEL® and INCOTHERM™ are registered trademarks of the Special Metals Corporation group of companies.

relevance to general applications requiring resistance to high temperature oxidation. Resistance to high-temperature corrosion results from an alloy's ability to form a dense adherent surface scale in the operating atmosphere. For iron and nickel alloys, chromium is added to impart corrosion resistance at elevated temperatures. The oxidation resistance of nickel as a function of chromium content has been widely studied.⁽¹⁻²⁾ As the chromium level increases in Ni-Cr alloys the oxidation resistance increases. Increasing the chromium not only increases the corrosion resistance but also, through solid solution strengthening, increases the high temperature strength. The effects of silicon addition upon the oxidation resistance of nickel-base and Fe-Ni-Cr alloys have been reported by others.³⁻⁶ The potential positive effects of rare earth or 'reactive metal' additions have been investigated as well.⁷⁻¹¹

EXPERIMENTAL

Exposures in air plus 5% water vapor involved cycling samples to room temperature once per week and were performed in electrically-heated horizontal muffle furnaces having ceramic tubes. Samples measured 7.6mm X 19mm X thickness (1.5-2mm) and were abraded through 120-grit SiC papers; samples were degreased in acetone prior to exposure. Samples were obtained from commercial sheet and plate stock produced by Special Metals Corporation. Table 1 shows the nominal composition for the alloys examined. Water vapor was added by bubbling air through a constant-temperature water bath and maintaining the temperature of transfer lines above the condensation temperature (33°C for 5% water vapor). Samples were weighed to the nearest 0.1 mg using an electronic balance.

Cyclic testing at 1200°C in oxygen was performed at Oak Ridge National Laboratory. Samples were alternated between exposure in a vertical muffle furnace in oxygen for two hours and cooling in ambient temperature air for 10 minutes. Specimens measured 10mm X 10mm X thickness (1.5-2mm). Samples were abraded using SiC papers through 600-grit and degreased in methanol and acetone. Samples were weighed after 75, 150 and 250 cycles to the nearest 0.01 mg, using an electronic balance.

Specimens were prepared for metallographic examination using conventional techniques. Mounted samples were polished to a 0.05 µm finish.

RESULTS AND DISCUSSION

Mass change and depth of oxidation results after exposure in air plus 5% water vapor at 1000°C are shown in Figures 1 and 2. The water vapor content was chosen in order to eliminate variation due to changes in humidity in a laboratory which does not have controlled humidity. Depth of oxidation data has not yet been obtained for the alloy TD sample exposed for the longest time, as it is still on-going. The results showed that all of the nickel-base alloys tested exhibit very respectable resistance to oxidation at this temperature. Long-term data for alloys 601 and TD show that the alloy TD possesses superior resistance. Alloy TB exhibited less oxidation depth than alloy 600, possibly benefiting from its 1.4% silicon level. Long term testing would be required to better define the relative performance of alloys HX and TC. Figures 3 and 4 show mass change and oxide penetration results after exposure in air plus 5% water vapor at 1100°C. Again, alloy TD exhibits significantly better performance than the alloy 601, and slightly better performance than alloys TC and HX. The lower-chromium alloys, TB and 600, exhibited higher oxidation rates. Figures 5-7 show photomicrographs comparing the microstructures of high silicon alloys TB, TC and TD after 1032 hours of exposure. Voiding is evident in the alloy TC cross section, but not in the alloy TD cross section. Mass change after exposure in air plus 5% water vapor at 1200°C is shown in Figure 8. Figure 9 shows depth of oxidation measurements.

Mass change and depth of oxidation results after cyclic exposure in pure oxygen at 1200°C are shown in Figures 10 and 11. Depth of oxidation measurements could not be reliably obtained from the alloy MA758 sample, as the cross section was not uniform from edge to edge. Notable differences in relative performance are revealed upon comparison of this data with that collected from exposure in air + 5% water vapor at 1200°C with cycling to room temperature once per week. The more rapidly cycling pure oxygen furnace environment produced a significantly higher rate of oxidation, as evidenced by both mass change and oxide penetration measurements, for all materials exposed with the exception of alloy TD. The alloy TB, having the same chromium level as alloy 600, with 1.4% silicon and 0.4% niobium, exhibited a much higher oxidation rate than the alloy 600. The silicon oxide subscale was fairly continuous in the alloy TB sample sectioned after 100 hours of furnace exposure (50 cycles). Other researchers have observed lack of spalling resistance under cyclic conditions in alloys which form continuous silica layers.^{1,2} Additionally, the 1.5% niobium addition in the alloy TB may have contributed to its poor behavior relative to the alloy 600. Figure 12 shows mass change results after exposure in air at 1100°C for experimental heats of alloys A and B. Samples in this one case were in the form of machined cylinders measuring approximately 7.6mm in diameter and 19mm in length, machined to a 32 microinch finish. The results show that the higher niobium heat exhibits a much higher rate of oxidation. The depth of oxidation measured after exposure was 0.0115" in the case of alloy A and 0.0275" for alloy B. Comparison of results for alloys TC and TD may reveal similar phenomena, as alloy TC contains 0.5% niobium.

Figure 13 shows EPMA line scans for alloy TC samples stopped and sectioned after 75, 150 and 250 cycles at 1200°C in pure oxygen. Figures 14 and 15 show SEM-EDS elemental maps near the surface of the 150- and 250-cycle samples. The 150-cycle sample exhibited a Cr/Ni oxide layer with a discontinuous network of silicon oxide fingers beneath. The 250-cycle sample possessed a dual outer scale, likely comprised of a $(\text{Ni,Cr})_2\text{O}_3$ inner layer and a $(\text{Ni,Cr})_3\text{O}_4$ thicker outer layer. The silica subscale was quite minimal in the 250-cycle sample, compared with the 150-hour sample, indicating advanced wastage of the depleted surface. Slight enrichment of niobium in the outer 200 microns, to greater than 1% near the surface, was evident in the line scans of the 75-cycle and 150-cycle samples. Niobium enrichment was less evident in the line scan of the 250-hour sample, as significant wastage had occurred resulting in removal of the originally niobium-enriched surface. Depletion of silicon and chromium was noted in all samples, to an approximate depth of about 600 microns and 400 microns, respectively, from the sample surface in each case. Reference to depth of oxidation measurements is recommended in interpreting these data, keeping in mind regression from the original sample surface. The chromium level near the surface of the 150-cycle sample had fallen to well below 10%, whereas the minimum chromium level measured for the 250-cycle sample was nearly 10%. Again this can be explained by rapid wastage of the depleted zone. Figures 16 and 17 show EPMA line scans and SEM-EDS elemental maps near the surface of alloy TD samples stopped and sectioned after 150 and 250 cycles. Depletion profiles for silicon and chromium were similar for both samples, and similar to those profiles observed for the alloy TC samples, at approximately 600 and 400 microns, respectively. The minimum chromium level measured near the surface of the 250-cycle sample was near 10%. Development of a rapidly growing outer scale and catastrophic wastage was not observed as in the case of the alloy TC, however. A significant network of discontinuous silicon oxide fingers was intact after 250 cycles, and the outer scale was observed to be rich in chromium and nickel. Some enrichment of molybdenum was observed in the outer 200 microns in each sample, with levels of about 4% near the surface. For comparison, Figure 18 shows SEM photomicrographs and EPMA lines scans for the alloy MA758 sample. Chromium depletion profiles extended to a depth of about 400 microns, but minimum chromium levels near the surface were maintained at well above 20%.

CONCLUSIONS

Alloy TD exhibits impressive oxidation resistance in comparison with other wrought chromia formers having similar chromium levels. Performance is thought to be enhanced by the presence of a discontinuous silicon oxide subscale, and by the presence of rare earth metal additions. Comparison of oxidation data from exposure in air plus 5% water vapor at 1200°C (cycling to ambient temperature in air once per week) and data from exposure in pure oxygen at 1200°C (cycling to ambient temperature every two hours) shows that all alloys tested in oxygen with more frequent cycling to ambient temperature experienced significant increases in oxidation rate except for alloy TD. The niobium additions in alloys TB and TC are thought to exert a detrimental effect upon oxidation resistance, possibly associated with slight concentration of that element near the sample surface.

REFERENCES

- 1.) N. Birks and H. Rickert, J. Inst. Met., 91, (1962-63): p. 308.
- 2.) C.S. Giggins and F.S. Pettit, Trans. Met. Soc. AIME, 245, 12(1969): p. 2495.
- 3.) D. L. Douglass and J. S. Armijo, Oxidation of Metals, 2, 2(1970): p. 207.
- 4.) H. E. Evans, et al., Oxidation of Metals, 19, 1(1983): p. 1.
- 5.) G. D. Smith, CORROSION/96, paper. no. 137, (Houston, TX: NACE International, 1996).
- 6.) G. B. Abderrazik, G. Moulin and A. M. Huntz, Oxidation of Metals, 33, 3/4(1990): p. 191.
- 7.) K. N. Stratford and J. M. Harrison, Oxidation of Metals, 10, 6(1976): p. 347.
- 8.) F. H. Stott, Materials Characterization, 28(1992): p. 311.
- 9.) H. M. Tawancy, Oxidation of Metals, 45, 3/4(1996): p. 323.
- 10.) S. B. Shendye and D. A. Downham, Oxidation of Metals, 43, 5/6(1995): p. 435.
- 11.) H. Liu, S. B. Lyon, and M. M. Stack, Oxidation of Metals, 56, 1/2(2001): p. 147.

Table 1. Nominal Composition of the Alloys Examined

Element	Alloy TD	Alloy TB	Alloy TC	Alloy 600	Alloy HX	Alloy 601	Alloy MA758	Alloy A [†]	Alloy B [†]
Ni	Bal	Bal	Bal	Bal	Bal	Bal.	Bal.	Bal.	Bal.
C	0.006	0.006	0.008	0.04	0.07	0.03	0.04	0.03	0.02
Al	---	---	---	0.2	0.2	1.4	0.3	---	---
Si	1.4	1.4	1.4	0.1	0.3	0.3	---	1.39	1.43
Co	---	---	---	---	1.5	---	---	---	---
Mn	---	---	---	0.3	0.5	0.3	---	---	---
Cr	22	15	24	15	21	22	28	15.1	15.4
Cu	---	---	---	0.1	0.3	0.2	---	---	---
Fe	0.1	0.1	0.1	9	19	16	0.3	0.28	0.07
Nb	---	1.5	0.5	---	---	0.1	---	0.88	1.9
Mo	3	---	---	0.1	8.5	0.2	---	---	---
Ti	---	---	---	0.3	---	0.4	0.5	---	---
Ce+La	0.04	0.04	0.04	---	---	---	---	0.008	0.008
Other	---	---	---	---	---	---	0.5	0.005 Y	0.003 Y

*Maximum

†Actual Chemistry

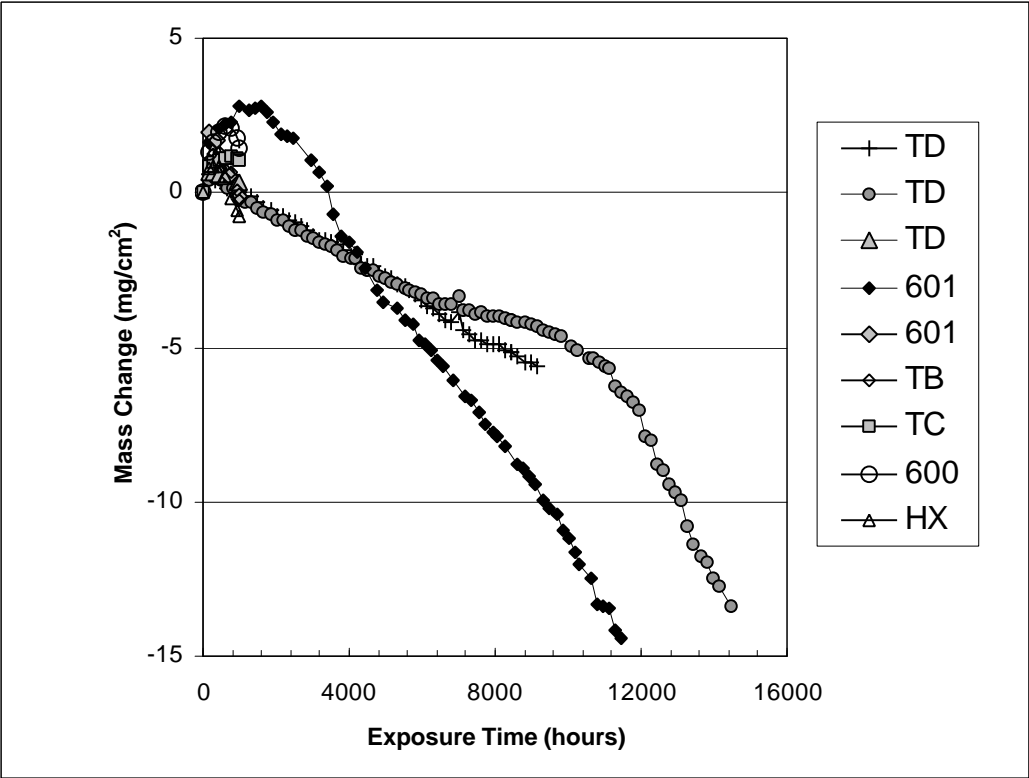


Figure 1. Mass change resulting from cyclic exposure (samples cycled to ambient temperature weekly and weighed) in air + 5% water vapor at 1000°C.

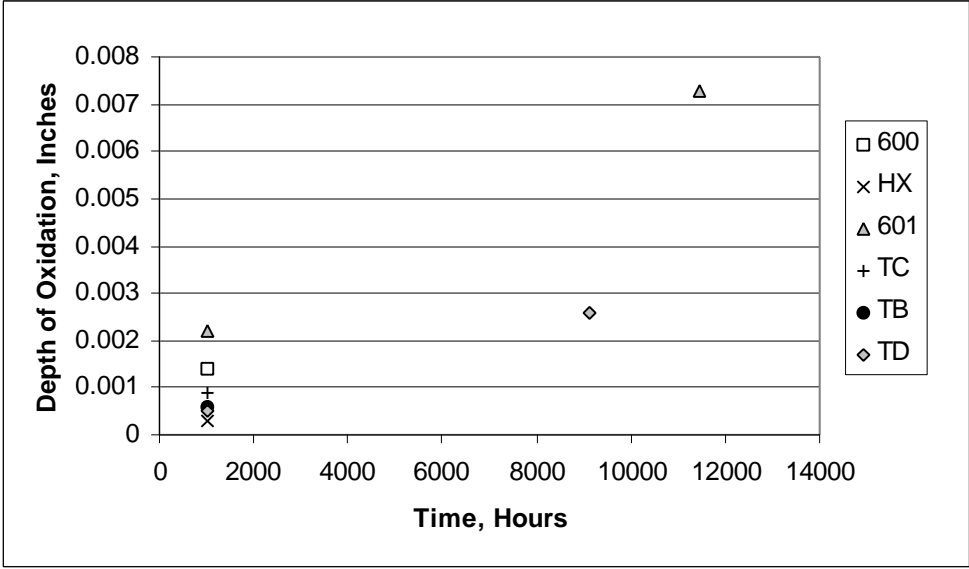


Figure 2. Depth of oxidation after cyclic exposure (samples cycled to ambient temperature weekly and weighed) in air + 5% water vapor at 1000°C.

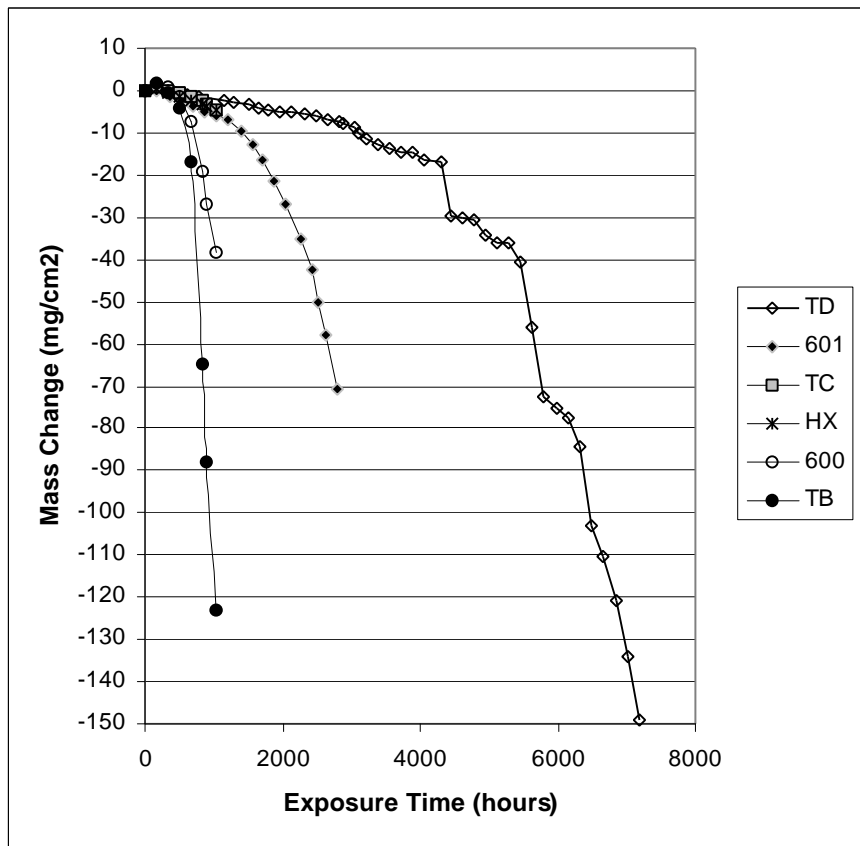


Figure 3. Mass change resulting from cyclic exposure (samples cycled to ambient temperature weekly and weighed) in air + 5% water vapor at 1100°C.

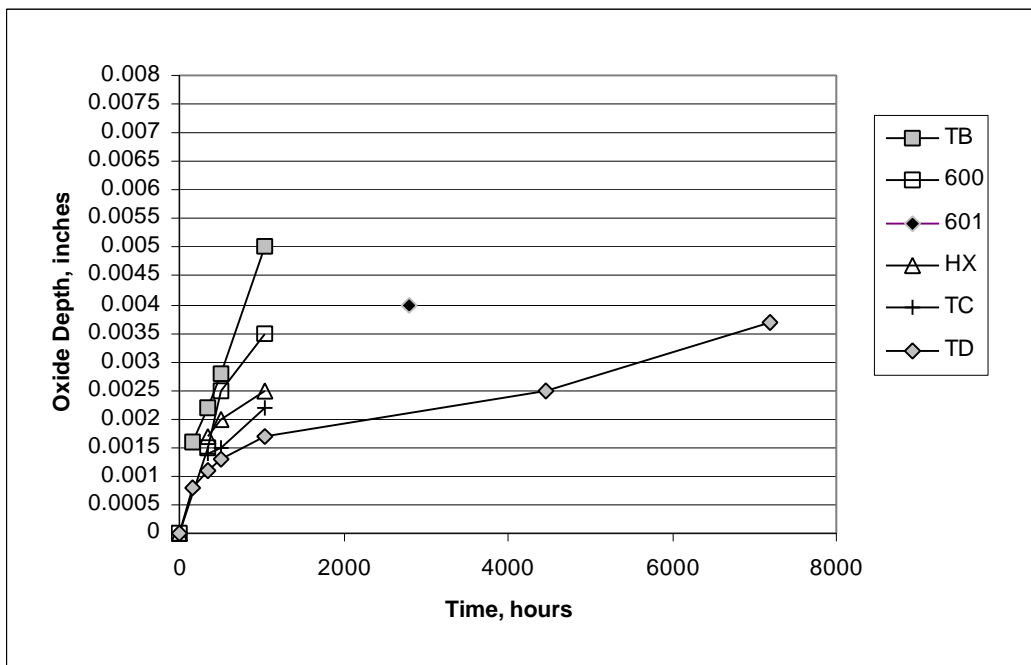


Figure 4. Depth of oxidation after cyclic exposure (samples cycled to ambient temperature weekly and weighed) in air + 5% water vapor at 1100°C.

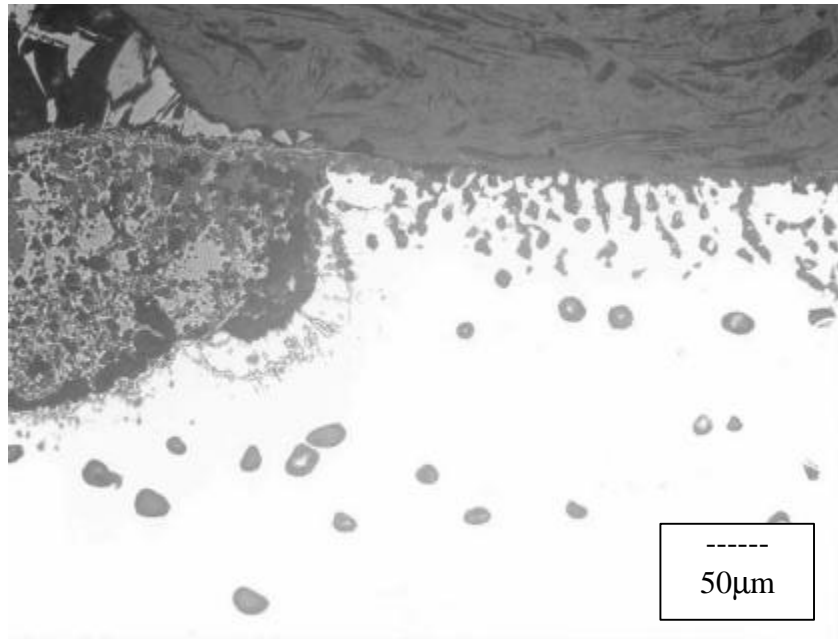


Figure 5. Photomicrograph showing a cross section from the alloy TB sample exposed for 1032 hours in air plus 5% water vapor at 1100°C (cycling to ambient temperature once per week). Sample unetched.

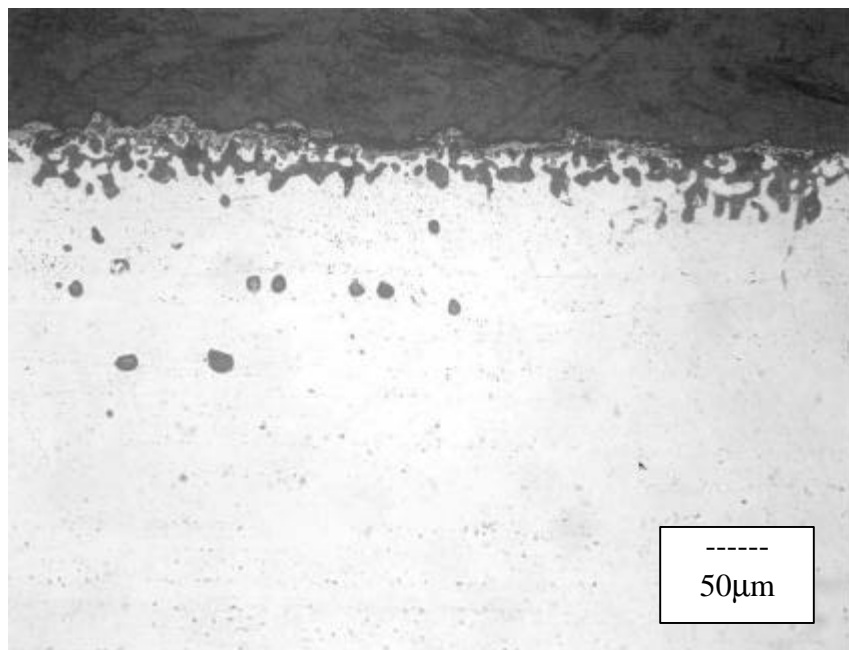


Figure 6. Photomicrograph showing a cross section from the alloy TC sample exposed for 1032 hours in air plus 5% water vapor at 1100°C (cycling to ambient temperature once per week). Sample unetched.

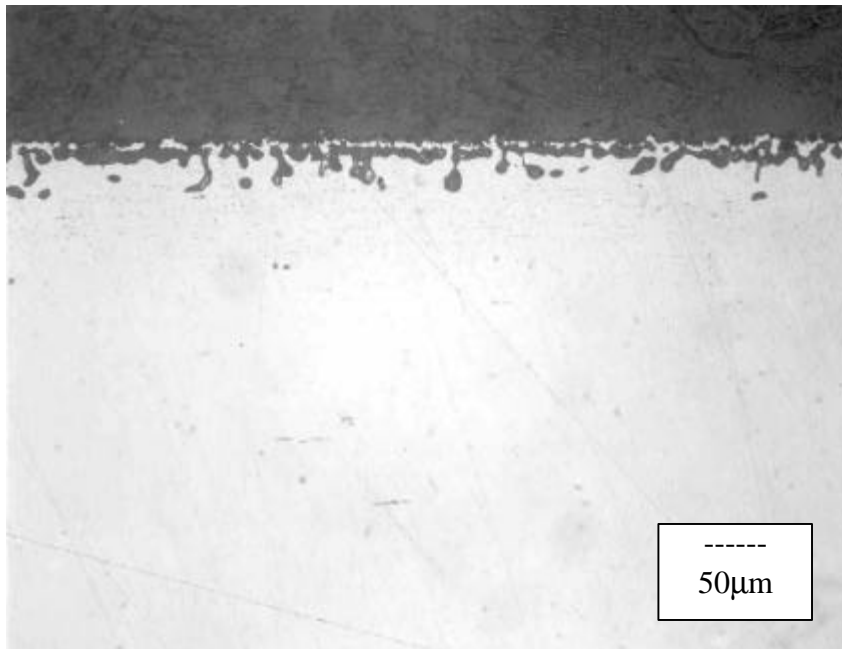


Figure 7. Photomicrograph showing a cross section from the alloy TD sample exposed for 1032 hours in air plus 5% water vapor at 1100°C (cycling to ambient temperature once per week). Sample unetched.

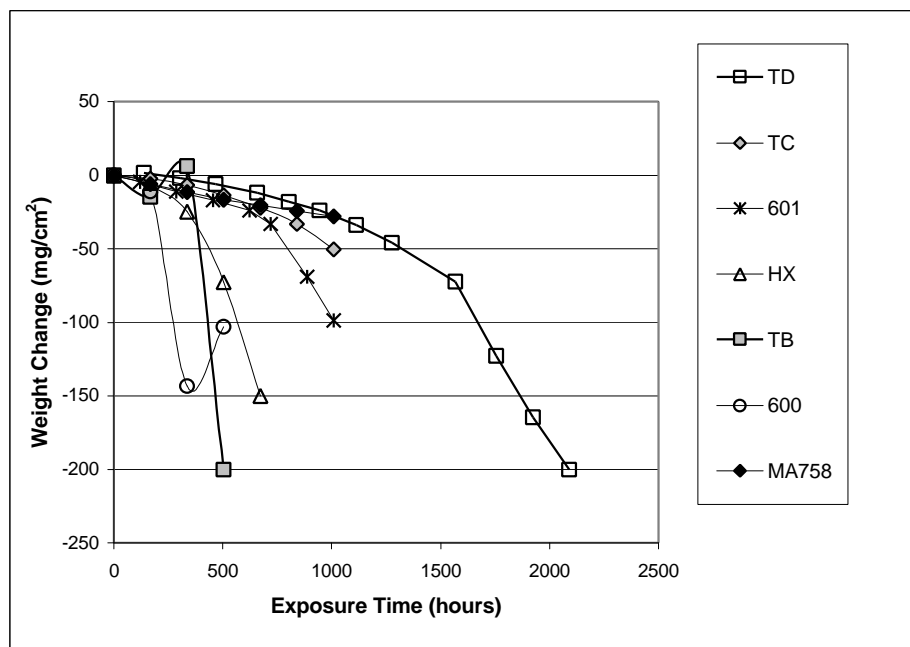


Figure 8. Mass change resulting from cyclic exposure (samples cycled to ambient temperature weekly and weighed) in air + 5% water vapor at 1200°C.

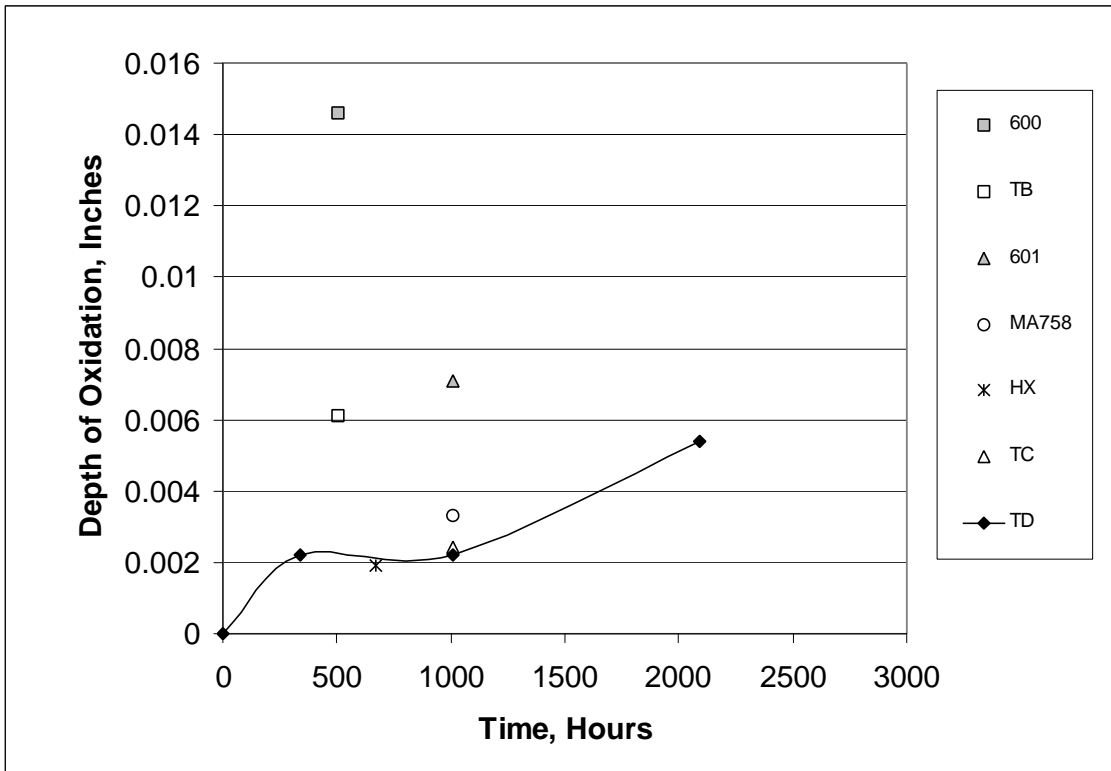


Figure 9. Depth of oxidation after cyclic exposure (samples cycled to ambient temperature weekly and weighed) in air + 5% water vapor at 1200°C.

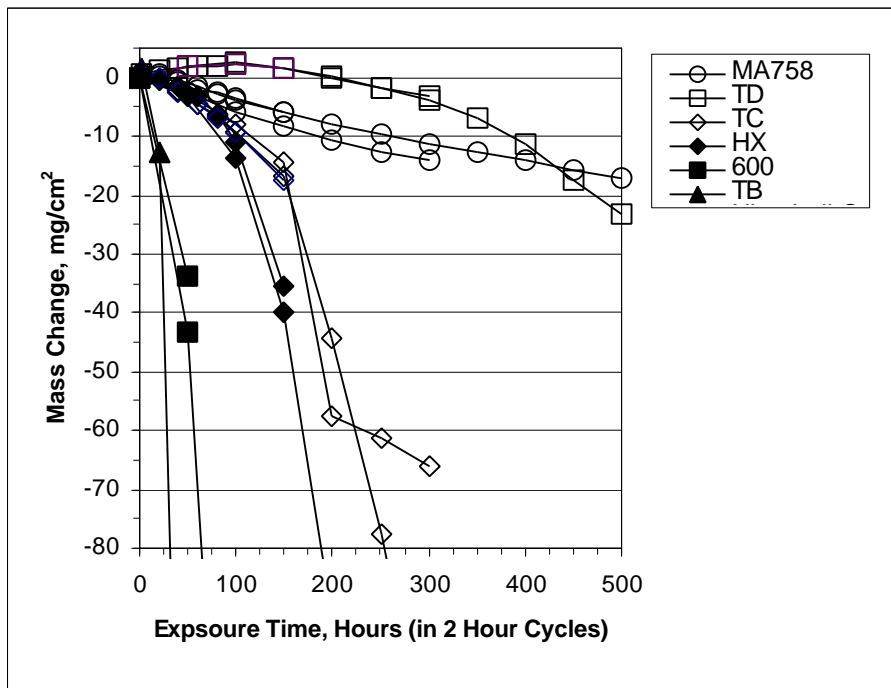


Figure 10. Mass change resulting from cyclic exposure in oxygen at 1200°C (one cycle=2 hours in furnace/10 minutes in ambient air).

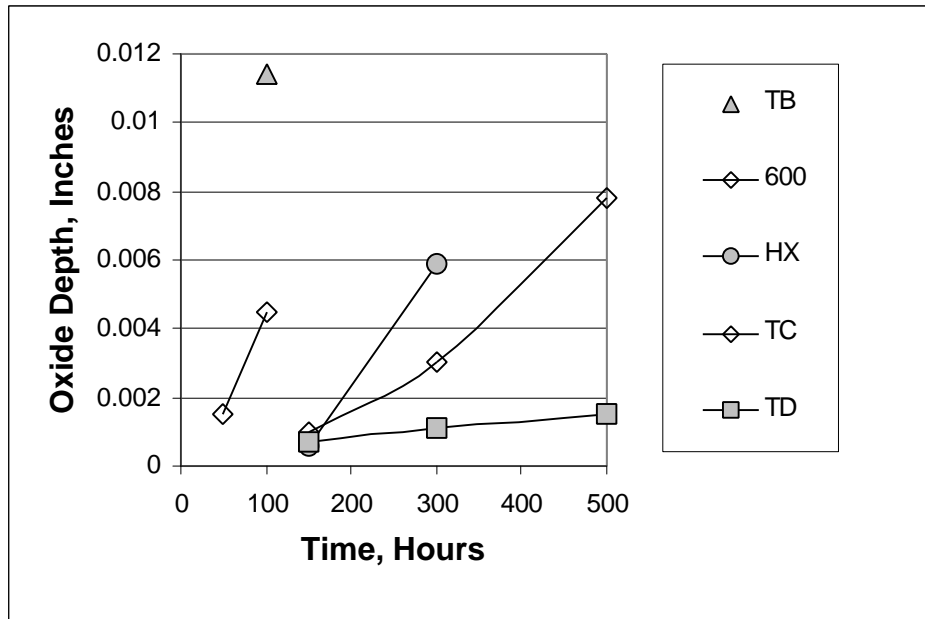


Figure 11. Depth of oxidation after cyclic exposure in oxygen at 1200°C (one cycle=2 hours in furnace/10 minutes in ambient air).

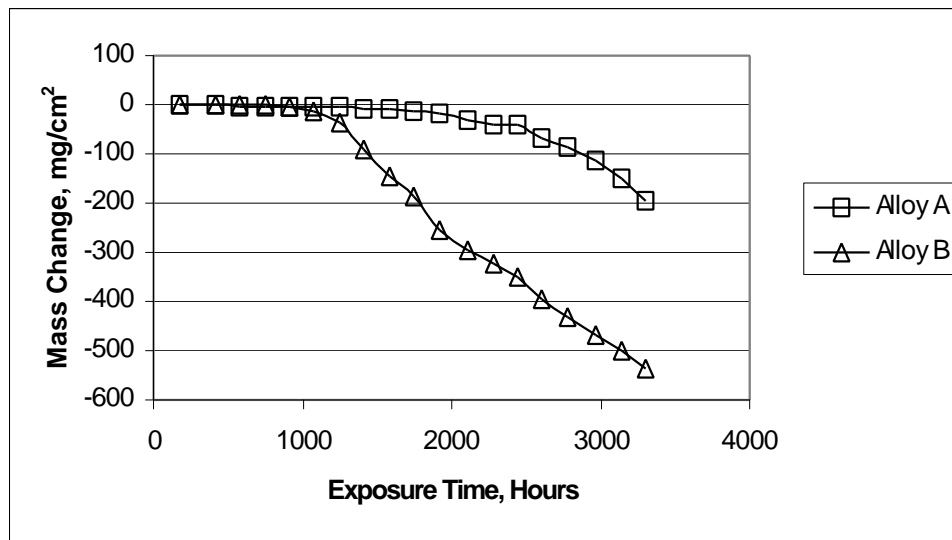


Figure 12. Mass change resulting from cyclic exposure (samples cycled to ambient temperature weekly and weighed) in air + 5% water vapor at 1100°C for alloys A and B. The results illustrate the effect of the higher niobium content of alloy B (1.9%) versus that of alloy A (0.88%).

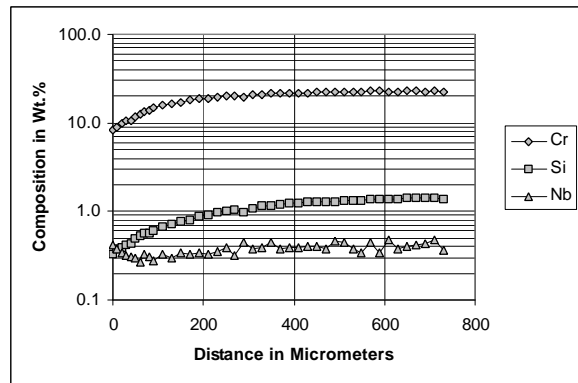
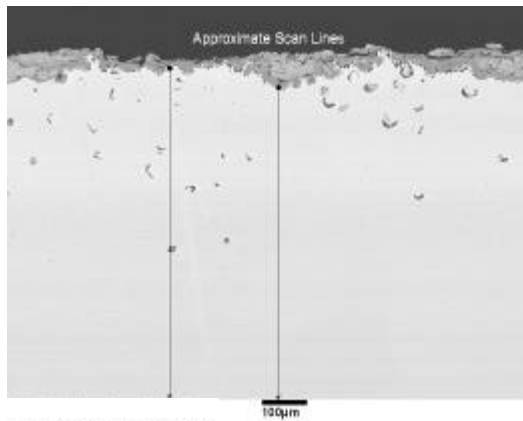
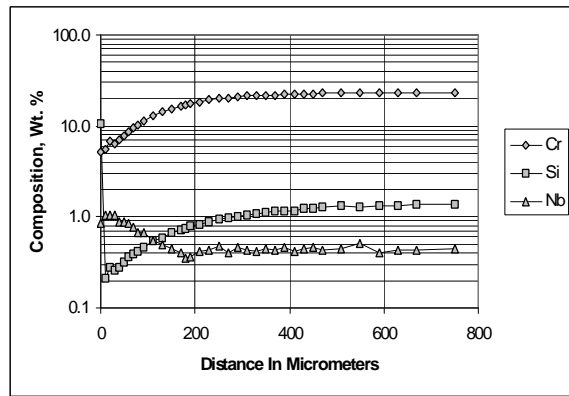
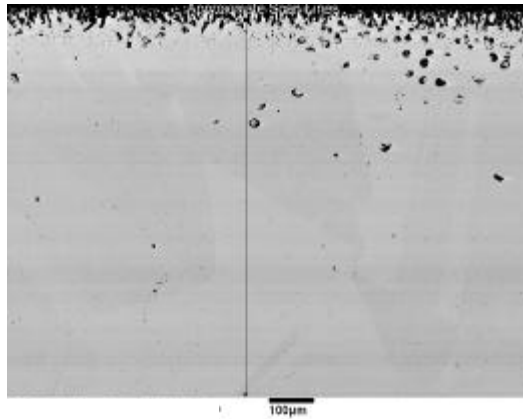
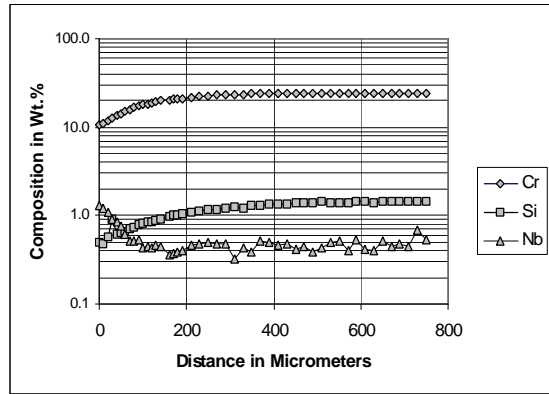
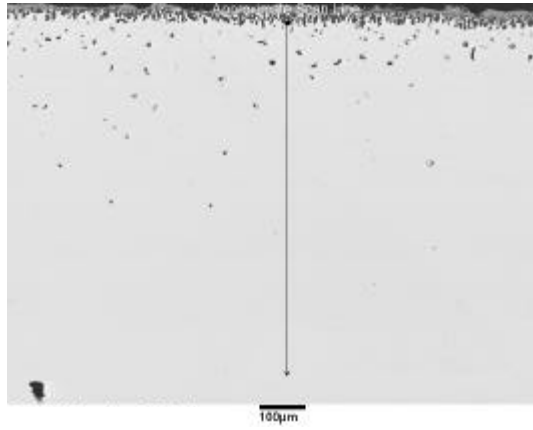
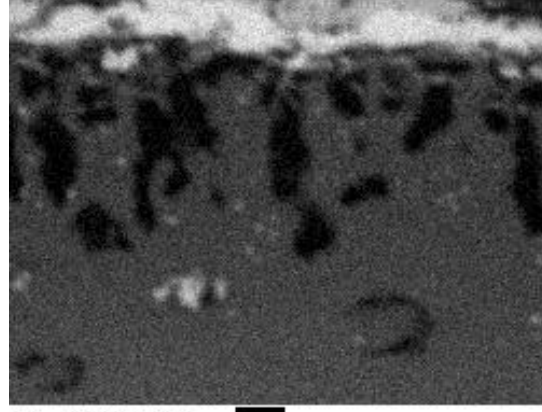
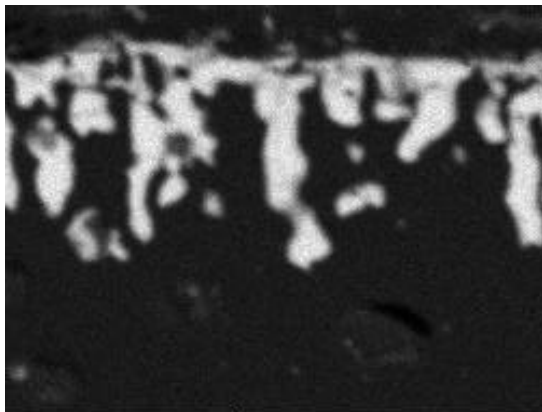
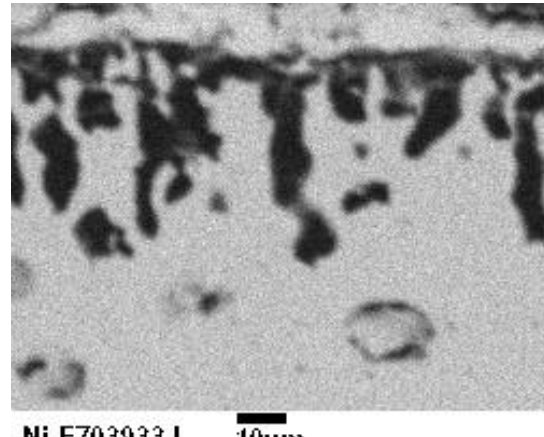
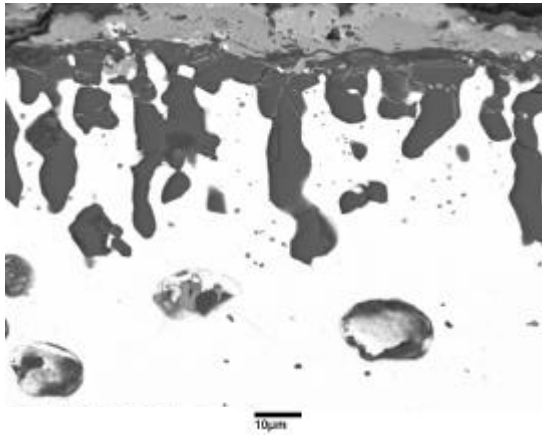
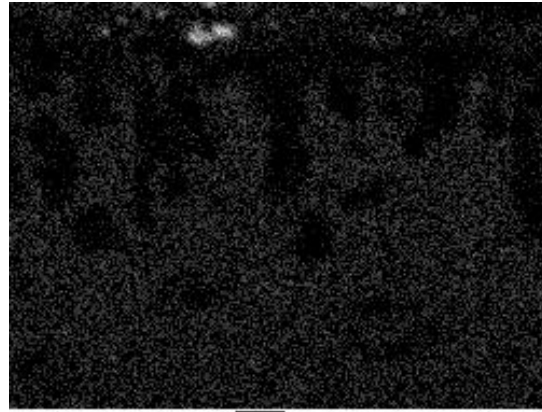
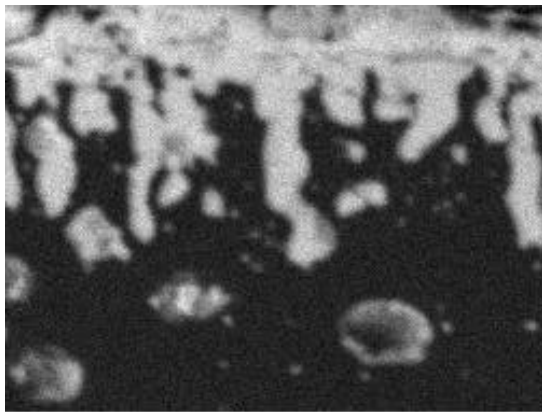


Figure 13. SEM backscatter photomicrographs showing cross sections of alloy TC samples exposed for 75 (top photo and chart), 150 (center photo and chart) and 250 cycles (bottom photo and chart) in oxygen at 1200°C (one cycle = 2 hours in furnace/10 minutes cooling in ambient air). The line in each photo indicates the path of the EPMA scan shown to the right (the line to the right in the case of the bottom photo).



Si EZ03933I 10µm

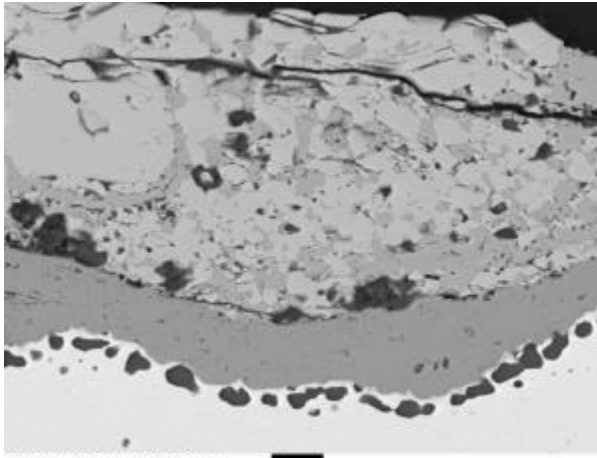
Ni EZ03933J 10µm



O EZ03933F 10µm

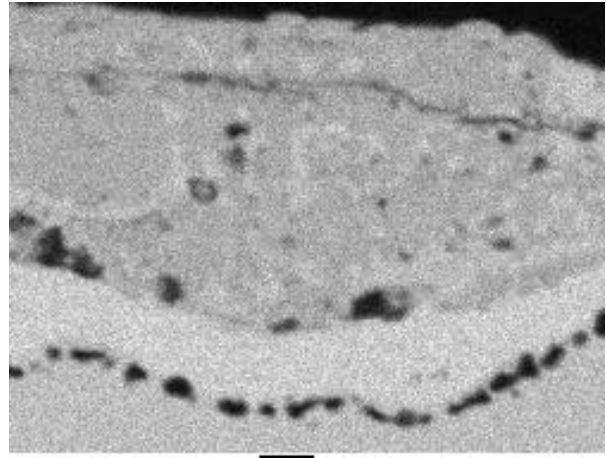
Nb EZ03933H 10µm

Figure 14. SEM-EDS maps showing elemental distribution near the surface of the alloy TC sample exposed for 150 cycles in oxygen at 1200°C (one cycle = 2 hours in furnace/10 minutes cooling in ambient air).



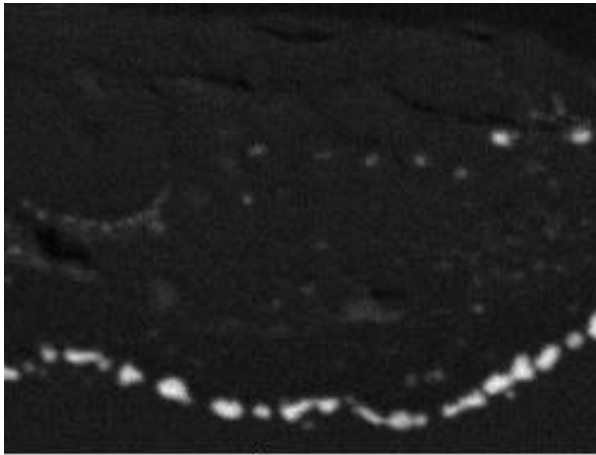
BS EZ03932D Alloy C 250 Cycles

10µm



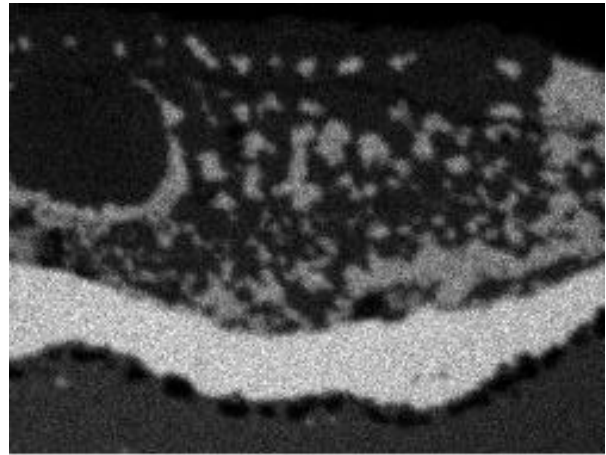
Ni EZ03932I

10µm



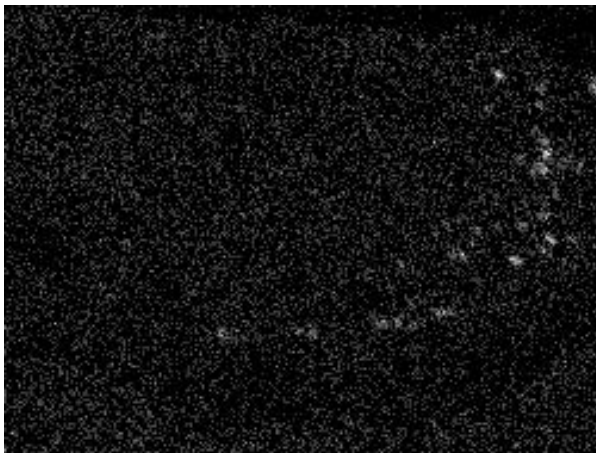
Si EZ03932H

10µm



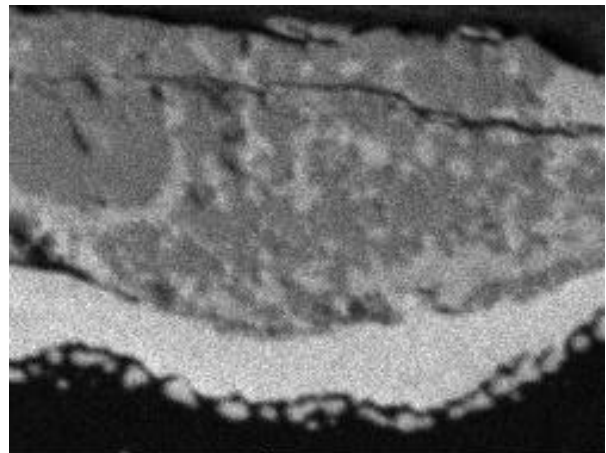
Cl EZ03932F

10µm



NB EZ03932G

10µm



O EZ03932E

10µm

Figure 15. SEM-EDS maps showing elemental distribution near the surface of the alloy TC sample exposed for 250 cycles in oxygen at 1200°C (one cycle = 2 hours in furnace/10 minutes cooling in ambient air).

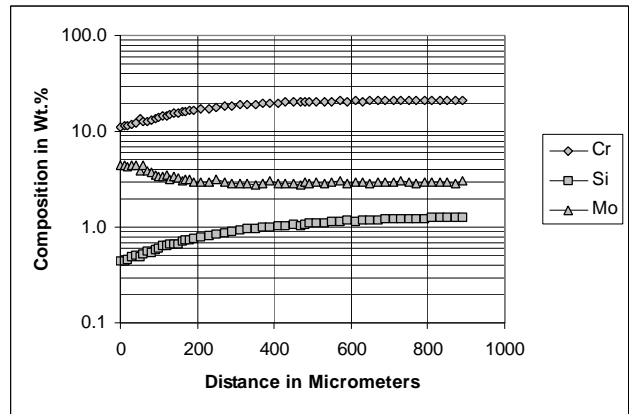
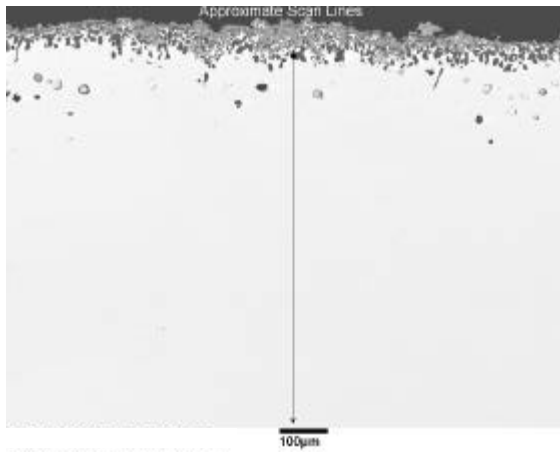
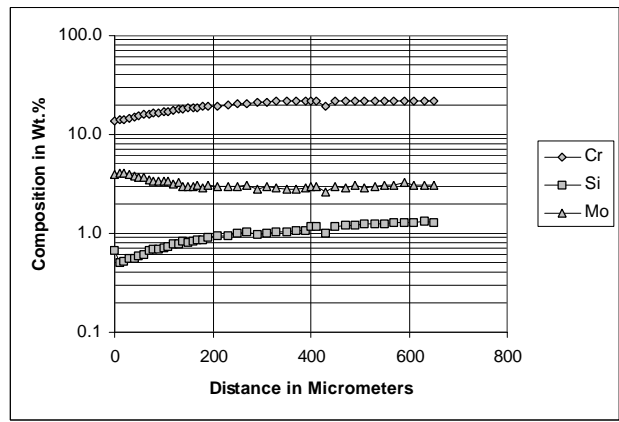
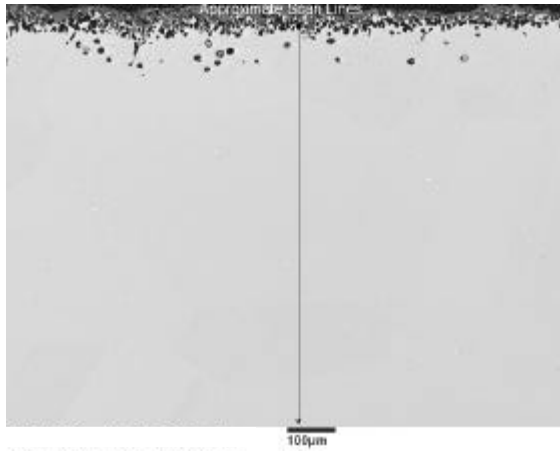
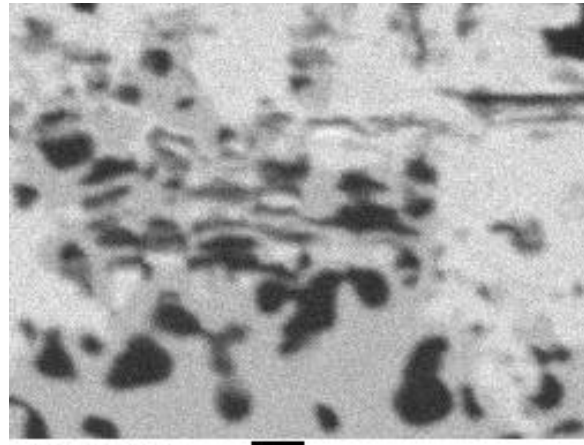
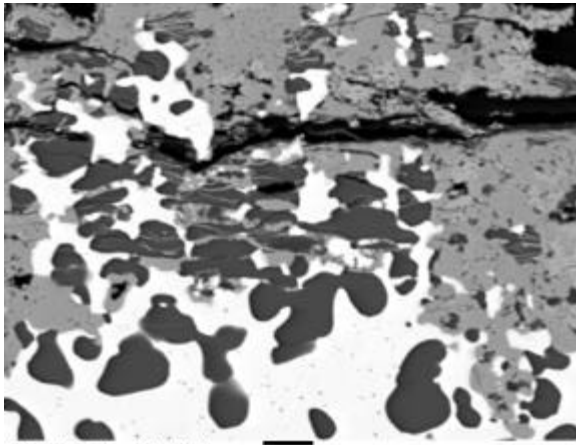
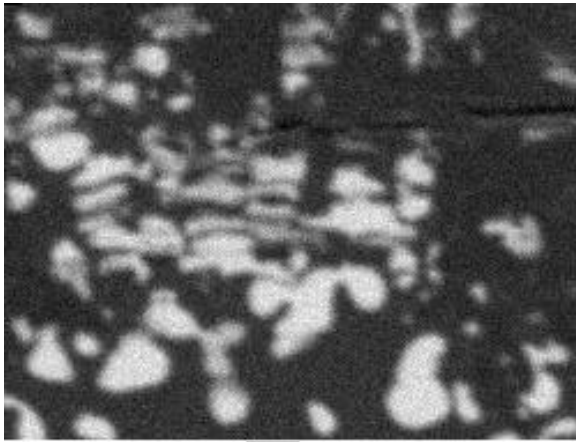


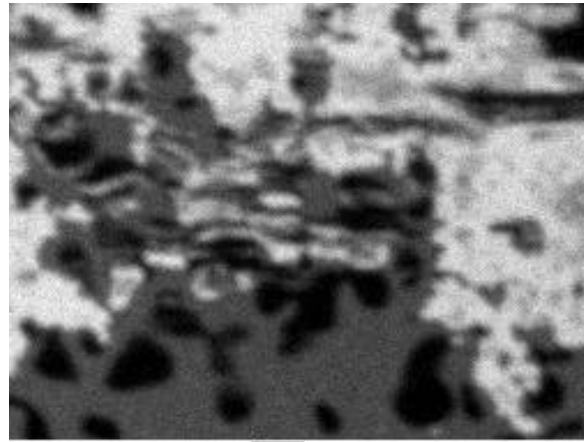
Figure 16. SEM backscatter photomicrographs showing the cross section of the alloy TD sample exposed for 150 (top) and 250 (bottom) cycles in oxygen at 1200°C (one cycle = 2 hours in furnace/10 minutes cooling in ambient air). The line in the photo indicates the path of the EPMA scan shown to the right.



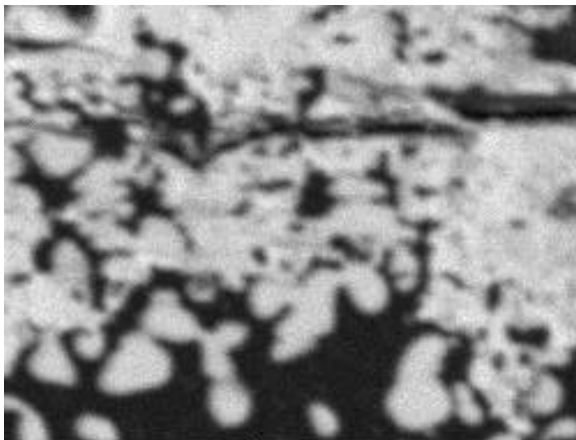
Ni EZ03936J 10µm



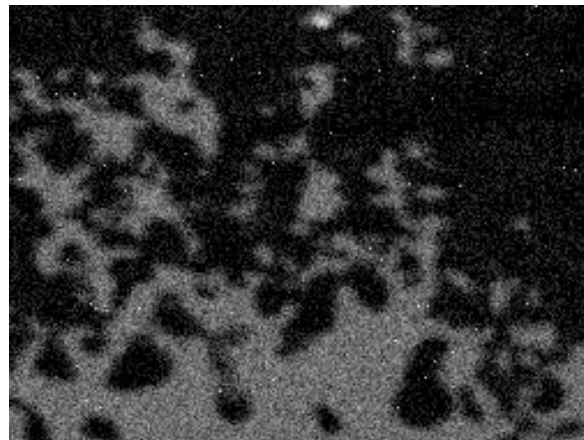
Si EZ03936I 10µm



Cl EZ03936G 10µm



O EZ03936F 10µm



Mo EZ03936H 10µm

Figure 17. SEM-EDS maps showing elemental distribution near the surface of the alloy TD sample exposed for 250 cycles in oxygen at 1200°C (one cycle = 2 hours in furnace/10 minutes cooling in ambient air).

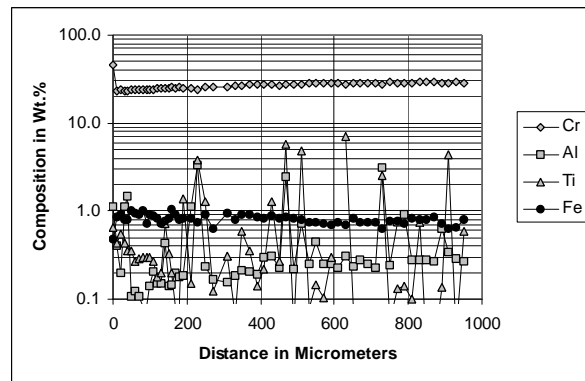
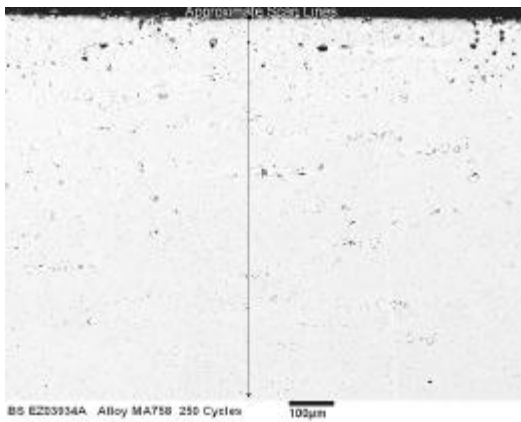
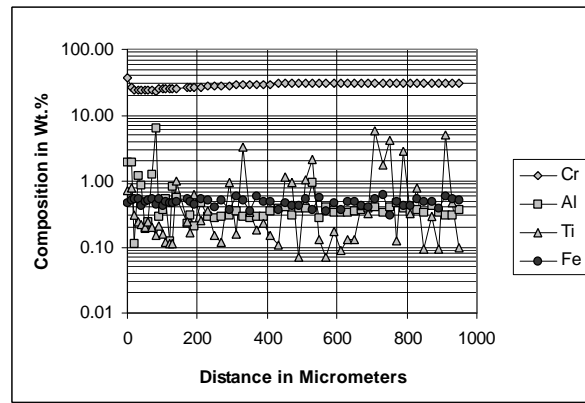
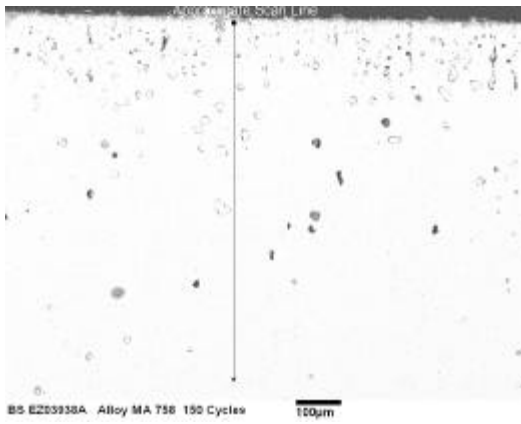


Figure 18. SEM backscatter photomicrograph showing the cross section of the alloy MA758 sample exposed for 150 (top) and 250 (bottom) cycles in oxygen at 1200°C (one cycle = 2 hours in furnace/10 minutes cooling in ambient air). The line in the photo indicates the path of the EPMA scan shown to the right.